

Co-precipitation method for the preparation of Mn-Zn Ferrite and study their Structural and Magnetic properties

W. A. Shatti*, Z. Mohammed Ali Abbas, Z. T. Khodair

University of Diyala, College of Science, Department of physics, Iraq

Ferrite nanoparticles were synthesized using the co-deposition method with pH = 12. This paper discusses the differences in composition and magnetic properties that contribute to the MnZn ferritic's properties. Samples were prepared, fabricated and annealed at two temperatures (600°C, 900°C). The crystal structure of the prepared samples was obtained using X-ray diffraction spectroscopy, Fourier transform infrared spectroscopy (FTIR) and field emitting electron microscopy (FESEM), respectively. The magnetic properties of the samples prepared by assay (VSM) were obtained and the magnetic and structural properties were discussed based on the changing temperature.

(Received March 4, 2022; Accepted June 28, 2022)

Keywords: Co-precipitation, Mn-Zn ferrite, Magnetic properties, VSM

1. Introduction

Magnetic nanoparticle systems have sparked a lot of interest in science research, particularly in physics and other fields [1,2]. Due to their numerous and important properties, the focus of new advanced studies has shifted to the synthesis of nanoparticles of metallic oxides, where a great need has emerged to create materials with a large area compared to their size, known as nanomaterials. These materials have unique properties, including the density of data storage for new devices. In a variety of applications, the use of nano-sized magnetic particles yields positive results where the type of ferrite spinel has properties and applications that have attracted great interest. Manganese ferrite ($\text{MnZnFe}_2\text{O}_4$) is one of these materials, which was previously thought to be reversed spinel due to its composition, but was recently discovered to be 80% natural and 20% reversed spinel. It has a high magnetic and electrical permeability, which has sparked interest in microwave electronic storage and magnetic storage device applications. Many methods have been developed to obtain magnetic ferrite particles, but some methods have many drawbacks, such as large particle size, irregular shape, and impurities, which prevent further improvement in the performance of the resulting materials [3,4]. Some wet chemical processes, such as gel citrate solution [5,6], a hydrothermal method [7], micro-emulsion process [8], co-sedimentation technique [9], and solution atomization [10], the emulsion blasting, have been developed to overcome these drawbacks and meet the requirements of new applications. An explosive [11] has been considered to produce nano-iron with excellent magnetic properties. Manganese ferrite ($\text{MnZnFe}_2\text{O}_4$) has received increasing attention for its remarkable magnetic properties, (low oppression, moderate saturation magnetization), along with good chemical stability, high permeability and mechanical toughness [12]. The high-density manganese ferrite was also characterized by its great importance for its use in technological applications and as basic raw materials in the manufacture of coils and transformers, as well as information and communication devices [13]. Increasing the calcination temperature leads to an increase in the size of the crystals. In recent years, this type of particle has been used in compact, lightweight and highly efficient power supply applications. [14,15].

* Corresponding authors: wafaa.satar80@gmail.com
<https://doi.org/10.15251/JOR.2022.184.473>

2. Materials and methods

2.1. Synthesis MnZnFe₂O₄ nanoparticles

Manganese ferrite nanoparticles [(MnZnFe₂O₄)] were prepared using co-precipitation method, which is one of the good methods for preparing ferrite. The materials (FeCl₃) (ZnCl₂) and (MnCl₂) were used as the basic material according to the following mathematical equation (1). Using a magnetic stirrer, the solutions were made by dissolving each ingredient individually in 50 ml of distilled water, then combining the solutions to obtain a homogeneous mixture. NaOH was used as a precipitating agent . The aqueous mixture was prepared at 0.3 M in order to obtain the required atomic percentage of the final product. After mixing the three primary materials solutions, sodium hydroxide was added to the precipitate by burette drop by drop to control the pH of the solution during the distillation process. During the mixing process, the magnetic stirrer was used at a constant temperature of 80 °C continuously for 2 hours to obtain good results for the reaction process and then the sufficient precipitation phase was observed, the reaction was stopped and the precipitate was allowed to settle to the bottom of the thermo glass beaker. After that, the sediment is cooled and then the top water is removed from the sediment using a simple straw and then the on-site washing process begins by removing water from the sediment by 10 to 20 times with ethanol and then at least twice with water and the precipitate is dried at room temperature and getting the powder Ferrite manganese.



The precipitate is then ground with a pestle to obtain a uniform powder containing fine nanoparticles of the desired substance after drying for 5-7 hours in a drying oven at a temperature of around 90°C.

3. Results and discussion

3.1. X-ray Difference

In this study the structural and structural properties of ferrite manganese zinc were discussed, particle size X-ray diffraction spectroscopy using Cu-Kα radiation ($\lambda = 1.5406 \text{ \AA}$) at room temperature was used and it was found that the analysis of the samples matches the structure of the cubic spinel of the particles. Then, the resulting peaks from the particle tests were experimentally matched with the theoretical peaks and indicators. The particle sizes were also calculated by the mathematical relationship of the Debye–Scherer equation (2) [16, 17]:

$$D = K\lambda / \beta \cos\theta \quad (2)$$

X-ray tests were carried out on the contained samples which were prepared by co-sedimentation method and what obtained after heat treatment. Figure 1 shows the XRD spectrum of ferrite for sample MnFe₂O₄, with all peaks in the figure depicted on the central face. Cube as per JCPDS Card No. 74-2403. where the positions of the diffraction and intensity peaks correspond to the XRD patterns, Good with standard MnFe₂O₄ ferrite crystals. Peaks can be indexed in the XRD pattern of the product perfectly Aspects (111), (220), (311), (400), (422), (511), (440) of the MnFe₂O₄ phase. No characteristic peak for the presence of impurities was observed confirming the purity of MnFe₂O₄. In addition, noting the relationship between the intensity of the diffraction peaks and the amount of MnZnFe₂O₄ samples tested Ferrite MnZnFe₂O₄ has a high degree of crystallinity, as evidenced by sharp characteristic peaks [18,19].

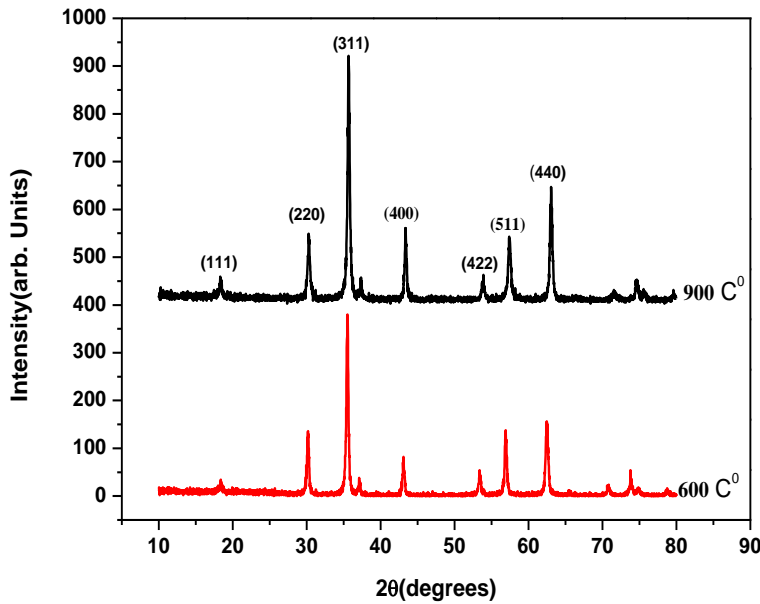


Fig. 1. XRD patterns at temperatures (600-900 °C).

Table 1. Shows the size difference of the prepared particles for each peak at annealing temperatures (600-900 °C).

(Lattices) (miller indices)	(Particle size (nm))	
	(annealed at 600 °C)	(annealed at 900 °C)
200	23	29
311	26	38
400	19	26
511	20	24
440	19	29

3.2. Nanostructured Analysis(FESEM)

The surface morphology of the as-prepared MnZ nFe2O4 magnetic nanoparticles was discussed using FESEM as shown in Figure (2 a-b).

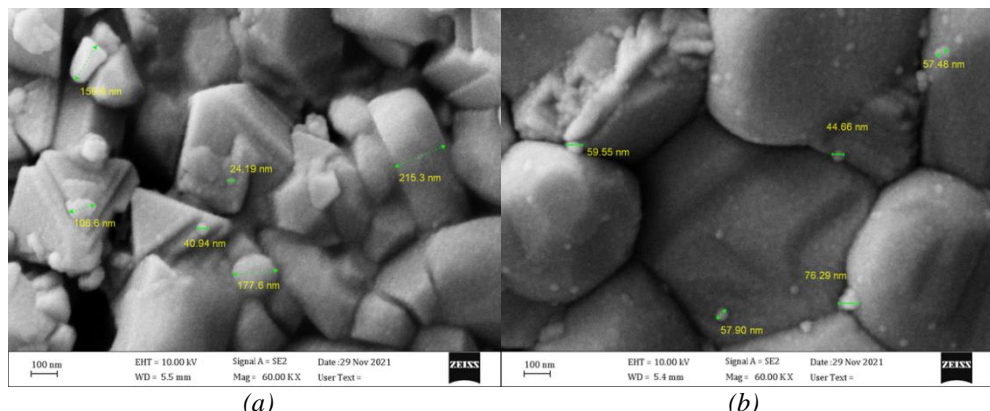


Fig. 2. Shows a FESEM technique for studying the morphology of Mn-Zn ferrites NPs.
a) 600 °C; b) 900 °C

The surface, as well as the size distribution of the prepared nanoparticles, have a clear appearance. From the figure, the average size of the prepared nanoparticles is estimated to be 46.8 nm. The grain size was also calculated using the (Scherrier equation) from the pattern of the X-ray diffraction spectrum and was found to be around 59.6 nm when compared to the value obtained from the FESEM image. It has been observed that nanoparticles agglomerate to some extent due to a lack of an effective stabilizing factor. The precipitated particles appear to agglomerate at (600) °C, but when the samples are annealed at 900 °C, the agglomeration decreases due to heat treatment. Samples prepared had scaly shapes, while those annealed at 900°C had cubic shapes. As a result of the heat treatment, linear particle growth occurred, resulting in cube-like structures at 900 °C, as shown in Figures 2(a) and 2(b) (b). As a result, it has a stricter requirement, which leads to smaller sizes[20], as shown in Table 2 shows.

Table 2. Average particle sizes calculated from XRD and FESEM.

Sample	Temp.°C	D(nm) XRD	D(nm) FE-SEM
MnZnFe ₂ O ₄	600	26	32
MnZnFe ₂ O ₄	900	38	53

3.3. Magnetic characterization

The magnetic properties of the prepared samples were studied using the VSM device, with the results indicating that samples have super magnetic properties through the Narrow hysteresis loop and that the magnetic field value for both samples, with the difference in temperature and the relationship between M - H for ferrite NPs NPs Mn-Zn, reached ± 10 kOe at room temperature. According to the results, all samples have different MS values, as shown in table 3. In the ferrite spinel structure, the spins in the A and B lattic modes rotate inversely to each other, as shown in Fig. 3a-b.

Table 3. VSM calculated results of Hc-M_S-M_r & S.

(Annealing temperature (°C)	(Coercivity) (Hc) (Oe)	(Remanent Magnetization) (Mr), (emu) /g	(Saturation Magnetization)(M _S) (emu)/ g	S=Mr/MS
600	124.212	0.8411	2.0241	0.4155
900	64.345	11.541	41.388	0.2788

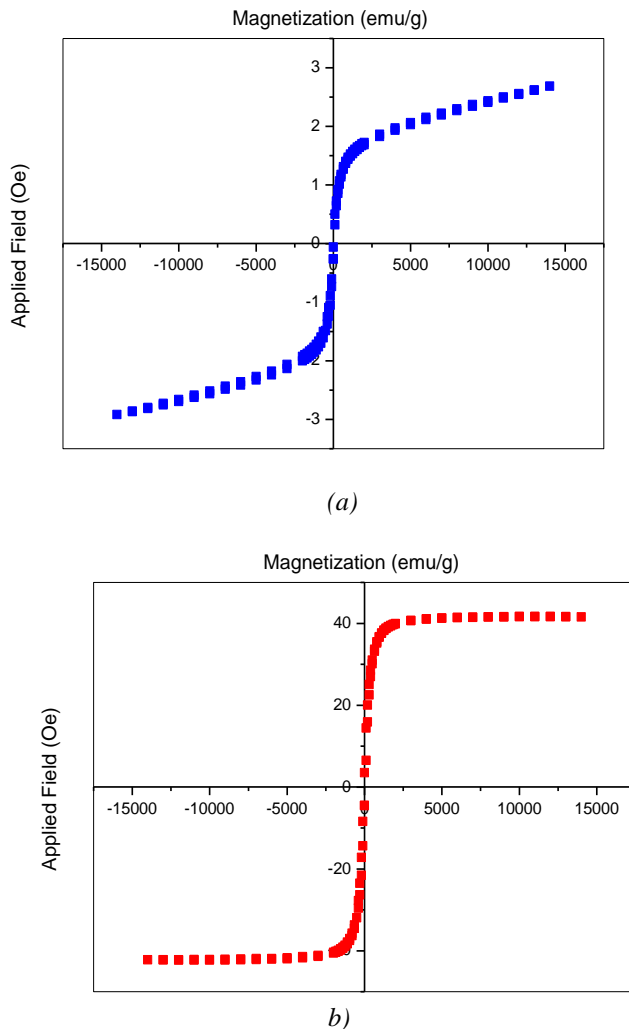


Fig. 3. Shows the hysteresis and hysteresis loop curve for particles prepared for ferrite at temperatures: a) 600 °C; b) 900 °C

4. FTIR Analysis

Figure 4 shows the results of the FTIR spectra (a-b). The patterns of hydroxyl vibrations are the set of peaks observed at (3500-4000 cm⁻¹) the group. The (O-H) group belongs to the organic group. With the C-H Series (Asymmetric), the existing double peak is shown at approximately 2350 cm⁻¹. In addition, it The strong peak at 1745 cm⁻¹ can be attributed to C = O Stretch, while the patterns at 1512 cm⁻¹, 1370 cm⁻¹ and 1210 cm⁻¹ could be due to C-O elongation, as shown by the intrinsic metal-oxygen bond vibrations that occur in MnFe₂O₄ Tetrahedral sites. Magnetism of the spinel structure The core is usually found at a depth of 600-570 cm⁻¹. Table No. 4 shows the range values for all samples. The variation in crystal size and temperature affects the distribution of cations between the tetrahedral and octahedral sites, as shown in the figure 4(a-b) which agrees with the researcher [21].

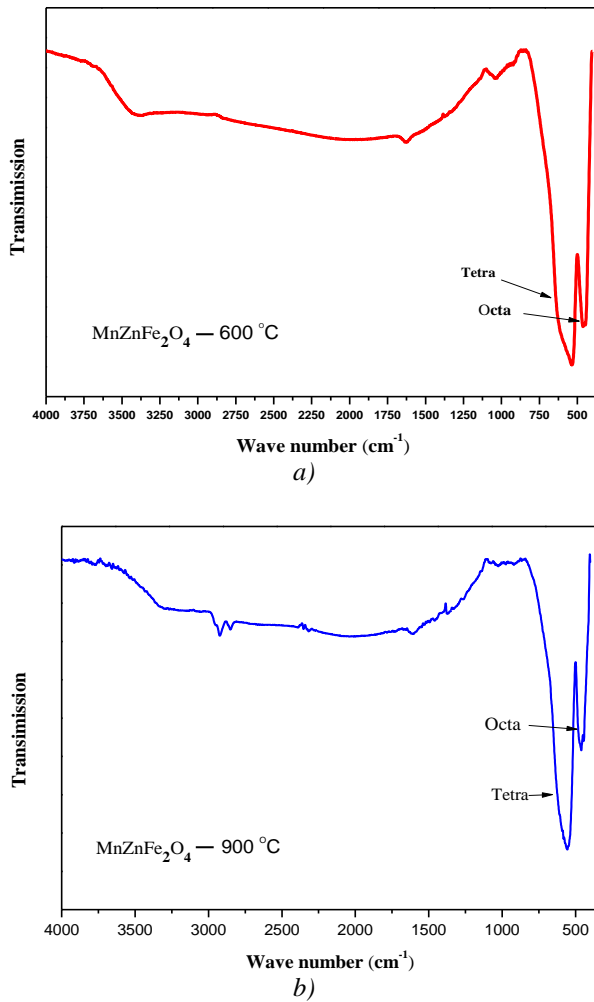


Fig. 4. FT-IR spectrum of ferrite for manganese and zinc at two temperatures: a) $600\text{ }^{\circ}\text{C}$; b) $900\text{ }^{\circ}\text{C}$

Table 4. of FTIR absorption ranges for zinc manganese ferrite at two degrees ($900\text{-}600\text{ }^{\circ}\text{C}$).

Annealing temperature ($^{\circ}\text{C}$)	$v_A(\text{cm}^{-1})$	$v_B(\text{cm}^{-1})$
600	425.67	431.7
900	451.59	482.1

5. Conclusion

$\text{MnZnFe}_2\text{O}_4$ is one of the most often used oxides, and it was synthesized using the co-precipitation method, followed by structural analysis using XRD, which revealed that the obtained MnFe_2O_4 particles are monodisperse, with an average size of nanoparticles (19-38) nm. The results of examining the structural properties of the screened samples showed a model of the nanostructure by understanding the structural properties of polycrystalline ferrite as well as the particle size and surface morphology of the samples using a set of FE-SEM images, which revealed that the samples have a spherical shape with narrow size distribution. Magnetic examinations of the as-prepared samples showed little residual coercivity and magnetization in addition to the presence of unobstructed super magnetic nanoparticles.

The magnetic moments within the nanoparticles tend to align in a specific direction known as the soft axis, resulting in the formation of a single domain magnetic nanoparticle. The samples'

infrared spectroscopy tests revealed two unique absorption bands in the ~561 and ~376 cm⁻¹ ranges. The expansion of the (A-O) site vibration causes the wave number to increase, whereas the expansion of the (B-O) site vibration causes the wave number to decrease. At the tetrahedral and octahedral positions, the force is constant.

References

- [1] G. Cao, Nanostructures nanomaterials Synthesis, Properties and Applications, Imperial College Press, (2004); <https://doi.org/10.1142/p305>
- [2] U. Evrim, Modern Surface Engineering Treatments 20, 185-208 (2013).
- [3] K. Dong-H. David E. Nikles, Christopher S. Brazel, Materials 3.7: 4051-4065 (2010); <https://doi.org/10.3390/ma3074051>
- [4] Y. Hong, et al., Biomaterials 31.13 : 3667-3673(2010); <https://doi.org/10.1016/j.biomaterials.2010.01.055>
- [5] L. Chao, et al., The Journal of Physical Chemistry B 104.6 (2000): 1141-1145; <https://doi.org/10.1021/jp993552g>
- [6] L. Chao, Z. John Zhang, Chemistry of Materials 13.6 2092-2096: (2001); <https://doi.org/10.1021/cm0009470>
- [7] R. Adam J., C. Liu, Z. John Zhang, The Journal of Physical Chemistry B 105.33: 7967-7971(2001); <https://doi.org/10.1021/jp011183u>
- [8] V. Christy R., Q. Song, Z. John Zhang, The Journal of Physical Chemistry B 108.47 : 18222-18227(2004); <https://doi.org/10.1021/jp0464526>
- [9] V. Christy R., Z. John Zhang, Journal of the American Chemical Society 125.32 : 9828-9833(2003); <https://doi.org/10.1021/ja035474n>
- [10] Y. Aria, et al., Nanotechnology 20.18 :185704(2009); <https://doi.org/10.1088/0957-4484/20/18/185704>
- [11] B. Aslubeiki et al., Journal of Magnetism and Magnetic Materials 322.19: 2929-2934(2010); <https://doi.org/10.1016/j.jmmm.2010.05.007>
- [12] T. Ulrich I. et al., Nano letters 7.8: 2422-2427(2007); <https://doi.org/10.1021/nl071099b>
- [13] C. Daniela et al., Inorganic chemistry 41.23: 6137-6146(2002); <https://doi.org/10.1021/ic025664j>
- [14] J. Paridaens, Magnetic and thermal analysis of the heating processes by magnetic hyperthermia in tumor treatment , Master's dissertation, Ghent university, (2017).
- [15] H. Seyed Hossein, et al., Journal of Alloys and Compounds 509.14: 4682-4687(2011); <https://doi.org/10.1016/j.jallcom.2010.11.198>
- [16] U. Evrim et al., Journal of colloid and interface science 550 (2019): 199-209; <https://doi.org/10.1016/j.jcis.2019.04.092>
- [17] Sh. Wafaa A., T.H. Mubarak, O. A. Mahmood, Diyala Journal For Pure Science 17.01 (2021); <https://doi.org/10.24237/djps.17.01.540C>
- [18] Y. Waseda, E. Matsubara, K. Shinoda, X-Ray Diffraction Crystallography: introduction, examples and solved problems, Springer Science and Business Media, (2011); <https://doi.org/10.1007/978-3-642-16635-8>
- [19] J. Smit, H.P.J Wijn, Ferrites: Physical Properties of Ferrimagnetic Oxides in Relation to Their Technical Applications , Philips, Eindhoven, (1959).
- [20] L. Kumar, P. Kumar, A. Narayan, M. Kar, International Nano Letters, vol. 3, no. 1, pp.1-12, (2013); <https://doi.org/10.1186/2228-5326-3-8>
- [21] D. Kotsikaua, V. Pankov, E. Petrova, V. Natarov, D. Filimonov, K. Pokholok, Journal of Physics and Chemistry of Solids, vol.114, pp.64-70, (2018)' <https://doi.org/10.1016/j.jpcs.2017.11.004>